OUKA
The University of Osaka
Institutional Knowledge Archive

Title	Anisotropic Transparency of Alkali-Treated Wood
Author(s)	Yagyu, Hitomi; Murayama, Hiryu; Ishioka, Shun et al.
Citation	Macromolecular Materials and Engineering. 2026, 311(2), p. e00389
Version Type	VoR
URL	https://hdl.handle.net/11094/104254
rights	This article is licensed under a Creative Commons Attribution 4.0 International License.
Note	

The University of Osaka Institutional Knowledge Archive : OUKA

https://ir.library.osaka-u.ac.jp/

The University of Osaka

Check for updates

Macromolecular Materials and Engineering

Macromolecular Materials and Engineering Open Access

www.mame-journal.de

RESEARCH ARTICLE OPEN ACCESS

Anisotropic Transparency of Alkali-Treated Wood

Hitomi Yagyu[1] | Hiryu Murayama[2] | Shun Ishioka[1] | Takaaki Kasuga[1] | Hirotaka Koga[1] | Yoshiki Horikawa[3] | Masaya Nogi[1]

[1]SANKEN (The Institute of Scientific and Industrial Research), The University of Osaka, Ibaraki, Osaka, Japan | [2]Research Institute For Sustainable Humanosphere, Kyoto University, Uji, Japan | [3]Institute of Agriculture, Tokyo University of Agriculture and Technology, Fuchu, Tokyo, Japan

Correspondence: Masaya Nogi (nogi@eco.sanken.osaka-u.ac.jp)

Received: 10 October 2025 | **Revised:** 4 January 2026 | **Accepted:** 19 January 2026

Keywords: alkali treatment | anisotropic structures | cellulose microfibril skeleton | delignification | holocellulose | transparent wood

ABSTRACT

This study elucidates the mechanism by which alkali treatment enhances the transparency of delignified wood, with a focus on the cellulose microfibril skeleton. Following delignification, the resulting material remains translucent due to light scattering from preserved lumens. Subsequent potassium hydroxide (KOH) treatment further removes hemicellulose and exchanges carboxyl-group counterions, which collectively soften the cell walls. This process allows the cellulose microfibril skeleton to undergo greater densification during drying, thereby reducing light scattering and yielding a highly transparent material without the need for polymer impregnation. We discovered that the inherent anisotropic structure of the wood's skeleton causes differential swelling between tangential and radial sections. The tangential sections, with their lower swelling ratio, undergo a more complete collapse of cell lumens, leading to higher density and superior transparency compared to the radial sections. This optical anisotropy, a direct consequence of the cellulose microfibril arrangement, was also evident in transparent wood-polymer composites. These findings highlight the fundamental role of the wood's underlying structure in determining its optical properties.

1 | Introduction

Wood is an opaque brown material because of the lumen and lignin within its cells. When the lignin is removed from wood, the pore structures of the wood cells are preserved and brown wood becomes a translucent white material owing to the scattering of light from the lumens. There are two procedures that can be used to prepare transparent wood. One method is the impregnation of trasparent polymer to the delignified white wood [1, 2], which was inspired by the transparent nanocomposites from bacterial cellulose or crab shells [3, 4]. Another method involves pressing wet brown wood under high temperatures so that the hygrothermally softened lignin compresses the lumens in the wood cells. During the 1920s and 1930s, this was reported as compressed wood, such as "lginostone" and "staypack," and their excellent mechanical properties, including their high strength & modulus, were widely known. Recently, it has been reported that careful pressing results in a transparent brown compressed wood [5]. Wood becomes opaque owing to light scattering from the lumens, so when the cavity is eliminated by resin impregnation or thermal deformation of the wood cells, the density of the wood increases, and the optical transparency is enhanced.

To produce transparent materials from wood without polymer impregnation or thermal deformation, it is necessary to nanofibrillate the pulp fibers [6–8]. In 2020, transparent wood without nanofibrillation was reported, in which delignified white wood was subjected to alkali treatment or 2,2,6,6-tetramethylpiperidinyl-1-oxyl (TEMPO)-mediated oxidation and then air-dried [9, 10]. Because of its attractive properties, transparent wood received much attention as an advanced wood material, and alternative methods have subsequently been proposed to prepare it, including lytic polysaccharide monooxygenase (LPMO) oxidation, dialdehyde oxidation, and ionic liquid

This is an open access article under the terms of the Creative Commons Attribution License, which permits use, distribution and reproduction in any medium, provided the original work is properly cited.

© 2026 The Author(s). *Macromolecular Materials and Engineering* published by Wiley-VCH GmbH

treatment [11–14]. Moreover, chemical crosslinking has been proposed to solve drying problems such as sample bending, warping, and cracking [15–17]. Transparent woods have been proposed for next-generation applications, such as device circuit boards, electromagnetic shielding, and chemiluminescent wood, and are attracting attention as new biomaterials [9, 18–21].

To improve the performance of transparent materials and make them more widely available, their transparency mechanisms must be understood. Delignified wood becomes translucent white after drying, as it retains its pore structure. By contrast, delignified wood with post-treatment becomes transparent after drying because its density increases owing to cell collapse during the drying process. There are four treatment methods for post-treatment—that is, TEMPO-oxidation, LPMO-oxidation, ionic liquid, and alkali methods—all of which increase the density and transparency of the delignified wood [9–11, 14]. In the former three treatments, they proposed the mechanism that the increase of density and transparency was caused by "capillary-driven self-densification" [10, 11, 14]. However, there has been no discussion on how to increase the transparency of the delignified wood after drying when using the alkali method.

Wood is a highly orthotropic material, meaning that its properties differ along three mutually orthogonal directions owing to its cellular orientation. Consequently, the same log can produce three types of boards—namely, tangential, radial, and cross-sectional boards. Owing to its orthotropic nature, each board exhibits different strengths, elastic moduli, and dimensional stabilities in water. However, their transparency and anisotropy have not yet been reported. Understanding how the intrinsic anisotropic structure of wood governs densification and optical transparency is not only of fundamental scientific interest but also provides essential design principles for wood-derived transparent materials. Clarifying such structure–property relationships is particularly important for materials engineering, where directional control of optical and mechanical properties is increasingly required. Therefore, in this study, we tested two hypotheses: that alkali treatment softens the cellulose microfibril skeleton, and that the anisotropy caused by the cellulose microfibril skeleton also affects transparency.

2 | Materials and Methods

2.1 | Translucent or Transparent Wood Without Polymer Impregnation

Native balsa wood was immersed overnight in distilled water and then used as the starting material. Balsa wood (*Ochroma pyramidale*) was cut to dimensions of 30 × 30 × 2 mm. Two types of wood sections were prepared—that is, radial (30 × 30 × 2 mm, L × R × T) and tangential (30 × 30 × 2 mm, L × T × R) sections (Figure 1). Their density was 0.08–0.12 g/cm^3. Five wood samples were delignified in a sealed petri dish using 2.5 g of sodium chlorite (80%), 0.83 mL of acetic acid, and 200 mL of distilled water at 80°C for 24 h without stirring, after which the samples were washed thoroughly using distilled water. Five delignified samples were immersed in 5% potassium hydroxide (KOH) solution at room temperature for 24 h without stirring before being washed thoroughly using distilled water.

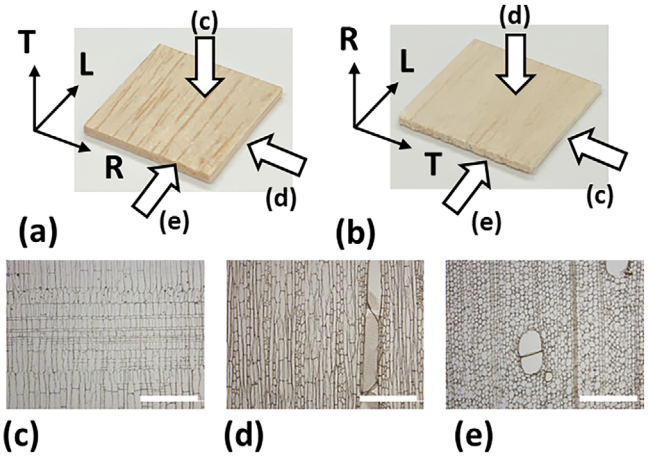

FIGURE 1 | (a) Radial section (30 × 30 × 2 mm, L × R × T), (b) tangential section (30 × 30 × 2 mm, L × T × R). Optical microscopic images in the (c) LR plane, (d) LT plane, and (e) RT plane. The scale bar is 500 μm.

Each sample was placed on a glass plate treated with a silane coupling agent and then covered with a metal mesh, absorbent paper, and a glass plate. They were dried at 30°C for 2–3 days under 5 kPa pressure and then stored at a relative humidity (RH) of 13%.

2.2 | Polymer-Impregnated Transparent Wood

Wet delignified KOH-treated wood was immersed in 50%, 60%, 70%, 80%, 90%, and 95% ethanol for 10 min each before being immersed in pure ethanol for 10 min, three times. The ethanol-immersed samples were dipped in acrylic resin (A-BPE-10, Shin–Nakamura Chemical Co., Ltd.) with 2 wt.% 2-hydroxy-2-methylpropiophenone photoinitiator (Nacalai Tesque) under reduced pressure for 6 h [22, 23]. The acrylic resin was selected because its refractive index (n = 1.536) is close to that of cellulose, which helps suppress interfacial light scattering and enhances optical transparency [23]. The acrylic resin impregnation was repeated five times. The resin-impregnated samples were polymerized under UV light until cured.

2.3 | Lignin, Cellulose, and Hemicellulose Content

In the native balsa wood, delignified wood, and KOH-treated wood, the lignin content was determined by the amount of sulfuric acid-insoluble Klason lignin. The classical method for the quantitative determination of lignin is based on Klason's technique involving hydrolysis with 72% sulfuric acid. In this procedure, the lignin remains as an insoluble residue and is recovered by filtration and gravimetrically determined.

In the native balsa wood, the holocellulose content was determined using Wise's sodium chlorite method. Here, 1 g of native balsa wood was applied to a cyclic treatment three times with 0.4 g of sodium chlorite (NaClO2), 0.08 mL of acetic acid, and 60 mL of distilled water at 70°C–80°C for 1 h. During this procedure, the holocellulose remains as an insoluble residue, which is recovered by filtration and gravimetrically determined. In the delignified wood and delignified KOH-treated wood, the

14392054, 2026, 2, Downloaded from https://onlinelibrary.wiley.com/doi/10.1002/mame.202500389 by The University Of Osaka, Wiley Online Library on [11/02/2026]. See the Terms and Conditions (https://onlinelibrary.wiley.com/terms-and-conditions) on Wiley Online Library for rules of use; OA articles are governed by the applicable Creative Commons License

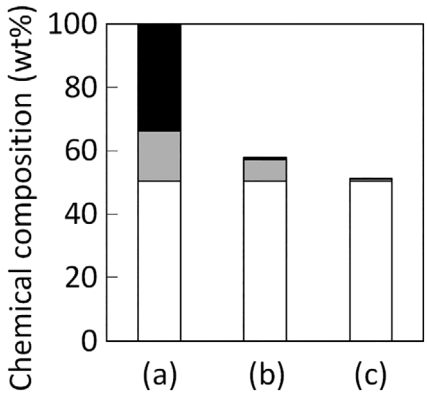

FIGURE 2 | Chemical composition percentages of cellulose (white), hemicellulose (gray), and lignin (black) for (a) native balsa wood, (b) delignified wood, and (c) delignified KOH-treated wood.

holocellulose content was determined from the initial and sample weights.

In the native balsa wood, delignified wood, and delignified KOH-treated wood, the cellulose content was determined to be alpha-cellulose, which is the fraction resistant to 17.5% sodium hydroxide (NaOH). The hemicellulose content was determined by subtracting the cellulose content from the holocellulose content [24].

2.4 | Characterization

The wood sections were observed using an optical microscope (BX61, Evident). Infrared spectra of radial-section delignified wood and radial-section delignified KOH-treated wood were measured using an FTIR spectrometer (Frontier TN, Perkin-Elmer Japan Co., Ltd.) equipped with an attenuated total reflection (ATR) attachment (Universal ATR, Perkin-Elmer Japan Co., Ltd.). All the spectra were obtained via the accumulation of four scans at a resolution of 4 cm^{-1} in the 1,500–1,800 cm^{-1} range. The total light transmittance was measured using a UV–vis spectrophotometer (U-3900, Hitachi High-Technologies Corp.). The carboxy content of the delignified radial section was determined using the electric conductivity titration method. The dried sample (3.0 g) was suspended in water (200 mL) and sufficiently stirred to be well dispersed. After 0.1 M NaCl (5 mL) was added, the pH value of the suspension was set to 2.8 with a 0.1 M HCl. 0.05 M NaOH solution then being added at a rate of 0.1 mL/min (up to pH 11) using a pH stat. The carboxylate content of the samples was determined from the conductivity and pH curves.

3 | Results and Discussion

The relationship between alkali treatment and transparency was first examined using a radial section of balsa wood. The native balsa wood contained 33.7, 15.9, and 50.4 wt.% lignin, hemicellulose, and cellulose, respectively (Figure 2a). In the delignified wood, the lignin was almost totally removed (0.5 wt.%), and the hemicellulose was reduced to less than half (6.9 wt.%), as shown in Figure 2. After KOH treatment, the hemicellulose content

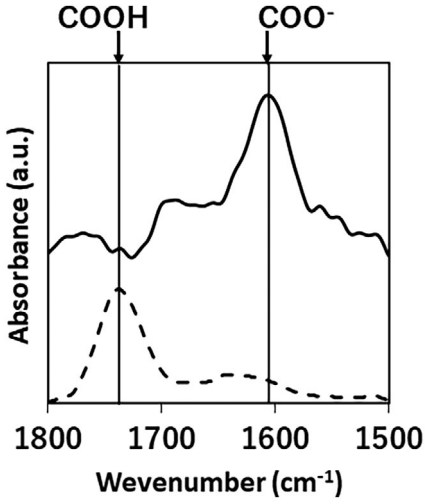

FIGURE 3 | FTIR spectra of the radial-section delignified wood (solid line) and radial-section delignified KOH-treated wood (dashed line).

decreased to 0.6 wt.%, and the delignified KOH-treated wood was comprised almost entirely of cellulose (Figure 2c).

Most lignin exists in the gaps between wood cell walls and bonds them together, whereas hemicellulose exists in wood cell walls and cross-links the cellulose microfibrils [25]. Therefore, in the delignified wood, the cellulose microfibrils were bridged by the residual hemicellulose, whereas in the delignified KOH-treated wood, the cellulose microfibrils were easily separated because of the relatively small amount of hemicellulose.

KOH alkali treatment not only removes the hemicellulose but also exchanges the counter ion types in the carboxyl group; notably, the counter ions that control the water swelling of cellulose materials (such as delignified wood and cellulose nanofiber films). Here, we prepared two cellulose nanofiber films (30 × 30 mm) with different counter ions—that is, H^+ or K^+ counter ions—using TEMPO-CNFs with 1.8 mmol/g of the carboxyl group. When these films were immersed in distilled water for 2 h, the area of the hydrophobic TEMPO-CNF film with H^+ counter ions expanded only 0.8%, whereas that of the hydrophilic TEMPO-CNF film with K^+ counter ions expanded 63.6%.

The delignified KOH-treated wood had different carboxyl-group counterions. For example, the delignified wood had a small amount of the carboxy group (0.3 mmol/mg), whose counter ions were H^+. During KOH treatment, the counter ions were exchanged with K^+ in the delignified KOH-treated wood (Figure 3). Consequently, when immersed in distilled water, the hydrophobic delignified wood did not swell and retained its shape (Figure 4, left), whereas the hydrophilic delignified KOH-treated wood swelled and lost its shape (Figure 4, right). Moreover, when the delignified wood was treated using an alkali, the hemicellulose was further removed, and the carboxyl-group counter ion was exchanged with K^+, making the wood cell walls softer and easier to deform.

In balsa wood, there are various size and shape cells, such as vessel elements (a large cell in Figure 5b), fibers (hexagonal or

14392054, 2026, 2, Downloaded from https://onlinelibrary.wiley.com/doi/10.1002/mame.202500389 by The University Of Osaka, Wiley Online Library on [11/02/2026]. See the Terms and Conditions (https://onlinelibrary.wiley.com/terms-and-conditions) on Wiley Online Library for rules of use; OA articles are governed by the applicable Creative Commons License

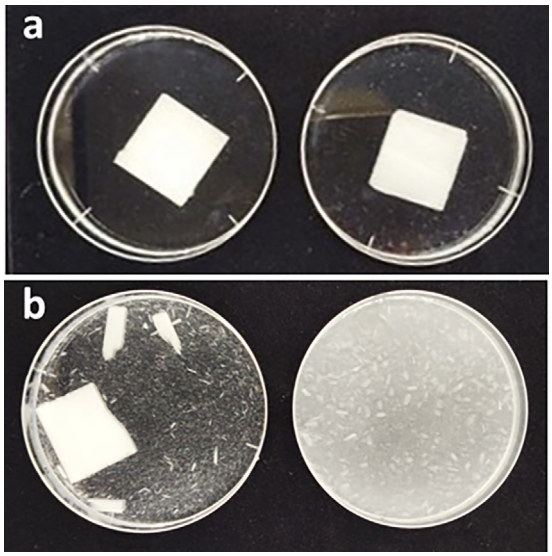

FIGURE 4 | Radial-section delignified wood (left) and radial-section delignified KOH-treated wood (right) in water for 10 s (a) and after 5 min stirring (b).

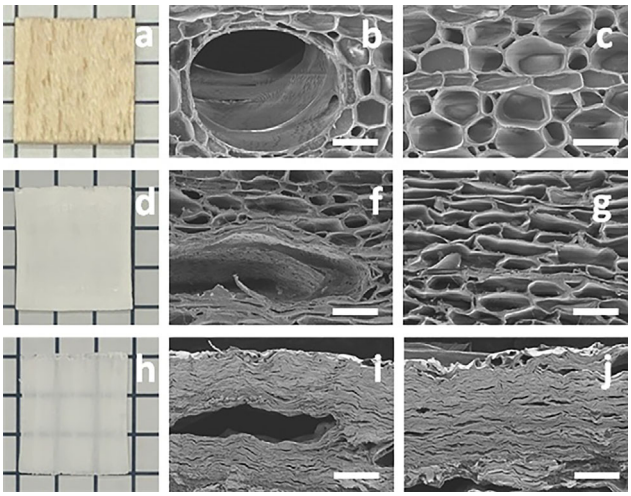

FIGURE 5 | Air-dried samples in the radial-section balsa wood (a), radial-section delignified wood (d), and radial-section delignified KOH-treated wood (h). Cross-section (RT plane) images of the radial-section native balsa wood (b,c), radial-section delignified wood (f,g), and radial-section delignified KOH-treated wood (i,j). The scale bar is 50 μm.

round cells in Figure 5b,c), and ray cells (rectangular cells in Figure 5c). Balsa wood has a very low density of 0.08–0.12 g/cm3, because of its thin cell walls (1–2 μm thick) and larger lumens (20–200 μm diameter). When incident light reaches the balsa wood, it is absorbed by the lignin components or scattered in the lumens. Thus, the 2-mm thick native balsa wood sample transmitted just 0.1% of the light at a wavelength of 550 nm (Figure 6). When the wet delignified wood was dried at 30°C, its thickness decreased to 0.26 mm, and its density increased to 0.54 g/cm^3.

In the delignified wood, the residual hemicellulose and carboxyl group with H^+ counter ions hold the cellulose microfibrils together. Thus, all the cells deformed into elliptical shapes, but all the lumens remained in the cavities (Figure 5f,g). Consequently, the delignified wood was translucent white with a total light transmittance of 16.0% at a wavelength of 550 nm (Figure 6). Conversely, in delignified KOH wood, the wood cell walls were easily deformed because most of the hemicellulose was removed, and the counter ion was exchanged from H^+ to K^+. The vessel elements were deformed into elliptical cavities (Figure 5i), whereas the lumens in the fibers and ray cells were deformed into flattened cavities (Figure 5j). Consequently, the dried delignified KOH-treated wood shrank to a thickness of 0.12 mm (density 0.71 g/cm3) and became transparent with a total light transmittance of 59.0% at a wavelength of 550 nm (Figure 6). This was a self-densification mechanism in which the delignified wood increased its density and transparency via alkali treatment.

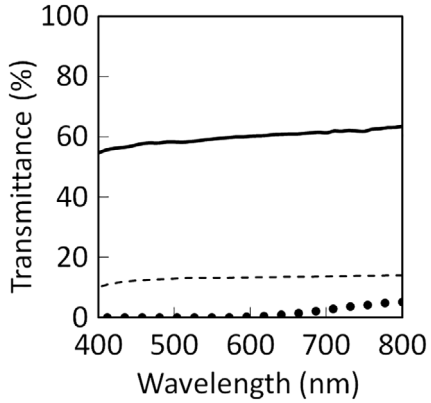

FIGURE 6 | Total transmittance in the radial-section native balsa wood (dotted line), radial-section delignified wood (dashed line), and radial-section delignified KOH-treated wood (solid line).

Wood is a 3D anisotropic material in the longitudinal, radial, and tangential directions (Figure 1). The longitudinal (L) direction is the direction of primary growth (length growth) in a tree, or the direction of the trunk axis. The radial (R) direction is perpendicular to the growth ring, and the tangential (T) direction is perpendicular to the trunk axis but tangential to the growth rings. After logging, highly orthotropic wood produces three different types of wood sections or boards—namely, radial, tangential, and cross-section boards. The radial section (LR plane) is the vertical plane from the pith at the center of the tree heading toward the bark (Figure 1a). The tangential section (LT plane) is the plane perpendicular to the trunk axis and tangential to the growth ring (Figure 1b). The cross-section (RT plane) is the plane perpendicular to the trunk axis.

We have discussed the relationship between alkali treatment and optical transparency using radial-section wood. In the cross-sectional specimens, there are boundaries between the earlywood and the latewood along the tangential direction. The amount of drying shrinkage is significantly different between earlywood and latewood because of their density gap. Therefore, both the delignified wood and the delignified KOH-treated wood had numerous cracks during drying, and they were unable to evaluate anything (Figure 7).

Here, we discuss the relationship between wood anisotropy and optical transparency using the radial and tangential sections. The thickness of the radial section is along the T-direction

14392054, 2026, 2, Downloaded from https://onlinelibrary.wiley.com/doi/10.1002/mame.202500389 by The University Of Osaka, Wiley Online Library on [11/02/2026]. See the Terms and Conditions (https://onlinelibrary.wiley.com/terms-and-conditions) on Wiley Online Library for rules of use; OA articles are governed by the applicable Creative Commons License

TABLE 1 | Swelling ratio from air-drying to water saturated conditions in the native balsa wood and delignified KOH-treated wood. The numbers in parentheses are the standard deviations.

	L-direction	R-direction	T-direction
Native balsa wood	0.20% (0.06%)	1.8% (0.55%)	6.0% (2.09%)
Delignified KOH treated wood after rinsing	0.36% (0.73%)	4.1% (1.13%)	13.3% (2.67%)

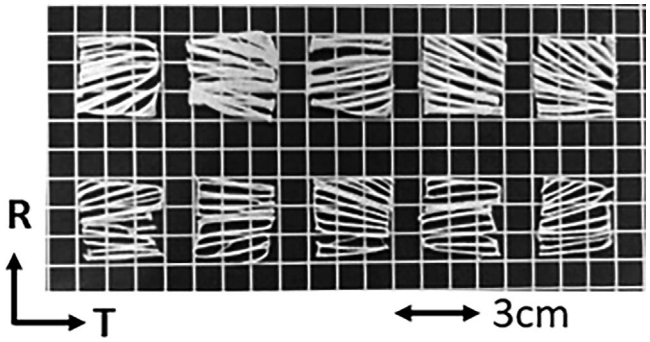

FIGURE 7 | After air-drying, the cross-section delignified wood (upper) and delignified KOH-treated wood (lower) with many cracks.

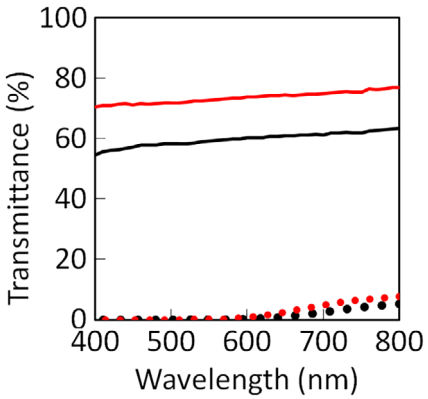

FIGURE 8 | Total transmittance in the radial-section (black dotted line) and tangential-section (red dotted line) native balsa wood, and in the radial-section (black solid line) and tangential-section (red solid line) delignified KOH-treated wood.

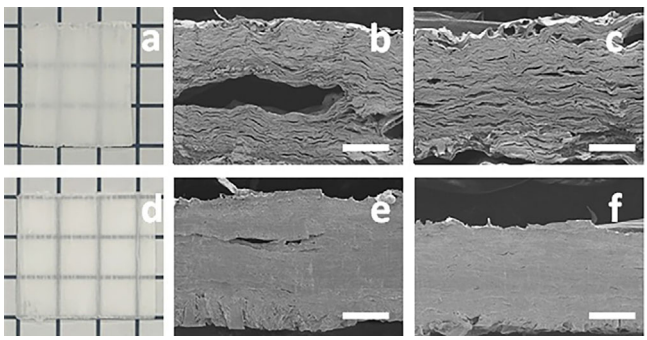

FIGURE 9 | Air-dried samples in the radial-section (a) and tangential-section (d) delignified KOH-treated wood. Cross-section (RT plane) images of the radial (b,c) and tangential-section (e,f) delignified KOH-treated wood. The scale bar is 50 μm.

(Figure 1a), and that of the tangential section is along the R-direction (Figure 1b). When the native balsa wood was immersed in the water, the thickness of the radial section swelled by 106.0%, whereas the thickness of the tangential section swelled by just 101.8% (Table 1). Because the delignified KOH-treated wood maintained its swelling anisotropy, the thickness of the radial section swelled to 113.3%, whereas the thickness of the tangential section swelled to just 104.1% (Table 1). Before drying, the wet tangential section exhibited higher transparency than that of the wet radial section owing to its thickness.

The native balsa radial and tangential sections exhibited the same total transmittance of 0.1% at 550 nm (dotted lines in Figure 8). When delignified, KOH-treated, and air-dried, the tangential section exhibited higher transparency than that of the radial section (solid lines in Figure 8, Figure 9a,d). When the more swollen radial section was dried, the vessel elements deformed into elliptical cavities (Figure 9b), and the lumens in the fibers and ray cells left traces (Figure 9b,c). Consequently, the treated radial section shrunk to a thickness of 0.12 mm (density 0.71 g/cm^3) and became transparent with a total light transmittance of 59.0% at a wavelength of 550 nm (black solid line in Figure 8). When the less swollen tangential section was dried, the vessel elements were deformed into flattened cavities (Figure 9e), and the lumens in the fibers and ray cells were so deformed that they could no longer be recognized (Figure 9e,f). As a result, the treated tangential section shrunk to a thickness of 0.08 mm (density 1.03 g/cm^3) and became transparent, with a total light transmittance of 69.1% at a wavelength of 550 nm (red solid line in Figure 8). The native balsa wood exhibited the same total transmittance in the radial and tangential sections, whereas the cellulose microfibril skeleton obtained by delignification and alkali treatment exhibited anisotropic transparency in the radial and tangential sections. It is evident that the wood anisotropy was derived from the cellulose microfibrils, and not from the lignin or hemicellulose.

In the delignified KOH-treated wood, the tangential-section dried wood was more transparent than the radial-section sample because the tangential section was thinner than the radial section. Consequently, the optical anisotropy of the wood/polymer composites were evaluated using the tangential and radial sections, with both the delignified KOH-treated tangential and radial sections being prepared accordingly. The delignified KOH-treated wet samples were subjected to a solvent exchange using an ethanol series to prevent dehydration. The immersed ethanol was then exchanged with acrylic resin, and transparent wood

14392054, 2026, 2, Downloaded from https://onlinelibrary.wiley.com/doi/10.1002/mame.202500389 by The University Of Osaka, Wiley Online Library on [11/02/2026]. See the Terms and Conditions (https://onlinelibrary.wiley.com/terms-and-conditions) on Wiley Online Library for rules of use; OA articles are governed by the applicable Creative Commons License

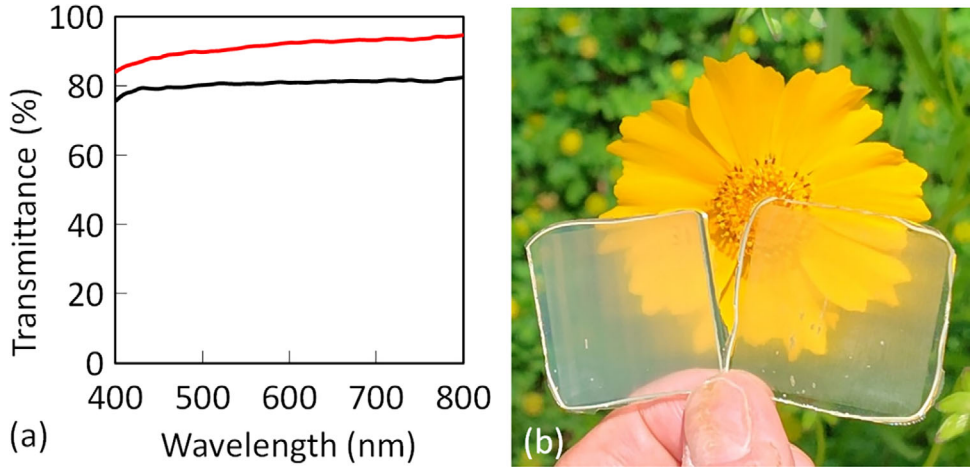

FIGURE 10 | Transparent wood composites reinforced with a transparent polymer. (a) Total transmittance in the radial-section (black line) and tangential-section (red line) delignified KOH-treated wood. (b) Transparent wood composites from the radial section (left) and tangential section (right).

composites were obtained via UV curing. Because the samples were carefully prepared to avoid dehydration or curing shrinkage, the tangential-section composites were thinner than the radial-section composites. Consequently, the total transmittance at 550 nm wavelength was 91.5% for the tangential-section composites and 81.0% for the radial section composites (Figure 10); because the tangential sections were thinner than the radial sections in the delignified KOH-treated wood, the tangential sections were also more transparent than the radial sections in the transparent wood composites.

4 | Conclusions

In this study, we examined the transparency improvement mechanism of alkali-treated delignified wood, and revealed that the tangential-section wood was more transparent than the radial-section wood owing to its swelling anisotropy. In the delignified wood, the residual hemicellulose and carboxyl group with H^+ counterions rendered the cell walls rigid. Therefore, even after drying, the delignified wood maintained the lumens in the wood cells and became white and translucent owing to the scattering of light from the air voids. When the delignified wood was treated with an alkali, the hemicellulose was further removed, and the counter ion of the carboxyl group was exchanged with K^+, resulting in the wood cell walls being softer and easier to deform. Consequently, after drying, the lumens of the fibers and ray cells were deformed into flattened cavities, and the vessel elements were deformed into elliptical cavities, rendering the dried, delignified KOH-treated wood transparent. The tangential and radial sections with lignin and hemicellulose exhibited different water-swelling ratios but the same light transmittance. When the lignin and hemicellulose were removed, they exhibited considerable swelling and optical anisotropy, with the swelling ratio being 4.1% of the thickness of the tangential section and 13.3% of the thickness of the radial section. Consequently, the vessel elements in the tangential section deformed into flattened cavities, whereas those in the radial section deformed into elliptical cavities; thus, in the dried delignified KOH-treated wood, the tangential-section samples exhibited higher transparency than that of the radial-section samples. This optical anisotropy was also evident in the transparent wood/polymer composites.

Author Contributions

The manuscript was written based on the contributions of all authors. All authors approved the final version of the manuscript. M.N. designed the study. All authors prepared the manuscript. H.Y., H.M., and Y.H. prepared samples. H.Y., H.M. and Y.H. performed the experiments. All authors analyzed the results and discussed the manuscript during its preparation. All authors discussed the results and implications and commented on the manuscript at all stages.

Acknowledgements

This study was partially supported by the JST CREST program (JPMJCR22L3 to M. N.).

Conflicts of Interest

The authors declare no conflicts of interest.

Data Availability Statement

The data that support the findings of this study are available from the corresponding author upon reasonable request.

References

1. S. Fink, "Transparent Wood—A New Approach in the Functional Study of Wood Structure," *Holzforschung* 46 (1992): 403–410, https://doi.org/10.1515/hfsg.1992.46.5.403.

2. Y. Li, Q. Fu, S. Yu, M. Yan, and L. Berglund, "Optically Transparent Wood from a Nanoporous Cellulosic Template: Combining Functional and Structural Performance," *Biomacromolecules* 17 (2016): 1358–1364, https://doi.org/10.1021/acs.biomac.6b00145.

3. H. Yano, J. Sugiyama, A. N. Nakagaito, et al., "Optically Transparent Composites Reinforced with Networks of Bacterial Nanofibers," *Advanced Materials* 17 (2005): 153–155, https://doi.org/10.1002/adma.200400597.

4. M. I. Shams, M. Nogi, L. A. Berglund, and H. Yano, "The Transparent Crab: Preparation and Nanostructural Implications for Bioinspired Optically Transparent Nanocomposites," *Soft Matter* 8 (2012): 1369–1373, https://doi.org/10.1039/C1SM06785K.

14392054, 2026, 2, Downloaded from https://onlinelibrary.wiley.com/doi/10.1002/mame.202500389 by The University Of Osaka, Wiley Online Library on [11/02/2026]. See the Terms and Conditions (https://onlinelibrary.wiley.com/terms-and-conditions) on Wiley Online Library for rules of use; OA articles are governed by the applicable Creative Commons License

5. T. Kasuga, A. Mizui, S. Ishioka, H. Koga, and M. Nogi, "Translucent Pure Wood Prepared via a Simple Compression Process," *Macromolecular Materials and Engineering* (2025): e00272, https://doi.org/10.1002/mame.202500272.

6. K. Abe, F. Nakatsubo, and H. Yano, "High-Strength Nanocomposite Based on Fibrillated Chemi-Thermomechanical Pulp," *Composites Science and Technology* 69 (2009): 2434–2437, https://doi.org/10.1016/j.compscitech.2009.06.015.

7. H. Fukuzumi, T. Saito, T. Iwata, Y. Kumamoto, and A. Isogai, "Transparent and High Gas Barrier Films of Cellulose Nanofibers Prepared by TEMPO-Mediated Oxidation," *Biomacromolecules* 10 (2009,): 162–165, https://doi.org/10.1021/bm801065u.

8. M. Nogi, S. Iwamoto, A. N. Nakagaito, and H. Yano, "Optically Transparent Nanofiber Paper," *Advanced Materials* 21 (2009): 1595–1598, https://doi.org/10.1002/adma.200803174.

9. Q. Fu, Y. Chen, and M. Sorieul, "Wood-Based Flexible Electronics," *ACS Nano* 14 (2020): 3528–3538, https://doi.org/10.1021/acsnano.9b09817.

10. K. Li, S. Wang, H. Chen, et al., "Self-Densification of Highly Mesoporous Wood Structure into a Strong and Transparent Film," *Advanced Materials* 32 (2020): 2003653, https://doi.org/10.1002/adma.202003653.

11. S. Koskela, S. Wang, L. Li, L. Zha, L. A. Berglund, and Q. Zhou, "An Oxidative Enzyme Boosting Mechanical and Optical Performance of Densified Wood Films," *Small* 19 (2023): 2205056, https://doi.org/10.1002/smll.202205056.

12. C. Chen, T. Zhou, Z. Wan, et al., "Insulative Biobased Glaze from Wood Laminates Obtained by Self-Adhesion," *Small* 19 (2023): 2301472, https://doi.org/10.1002/smll.202301472.

13. T. Zhou, J. Zhou, Q. Feng, et al., "Mechanically Strong, Hydrostable, and Biodegradable All-biobased Transparent Wood Films with UV-blocking Performance," *International Journal of Biological Macromolecules* 255 (2024): 128188, https://doi.org/10.1016/j.ijbiomac.2023.128188.

14. F. Chen, M. Ritter, Y. Xu, et al., "Lightweight, Strong, and Transparent Wood Films Produced by Capillary Driven Self-Densification," *Small* 20 (2024): 2311966, https://doi.org/10.1002/smll.202311966.

15. H. Sun, T. Ji, X. Zhou, et al., "Mechanically Strong, Transparent, and Biodegradable Wood-Derived Film," *Materials Chemistry Frontiers* 5 (2021): 7903–7909, https://doi.org/10.1039/D1QM00973G.

16. S. Wang, G. G. Mastantuoni, Y. Dong, and Q. Zhou, "Strong and Transparent Film of Naturally Aligned Softwood Holocellulose Fibers," *Carbohydrate Polymers* 347 (2025): 122722, https://doi.org/10.1016/j.carbpol.2024.122722.

17. H. Zhang, J. Chen, Y. Wang, et al., "Laminated Composites with an Ultra-High Cellulose Content Exhibit High Strength and Toughness," *Cellulose* 31 (2024): 7521–7530, https://doi.org/10.1007/s10570-024-06082-6.

18. Z. Li, W. Che, Y. Jiang, Y. Liu, X. Fang, and Y. Peng, "Strong, Hydrophobic, and Transparent Wood Film Decorated with MXene/Silver Nanowire for Electromagnetic Interference Shielding and Electrothermal Conversion," *Colloids and Surfaces A: Physicochemical and Engineering Aspects* 676 (2023): 132211, https://doi.org/10.1016/j.colsurfa.2023.132211.

19. W. Zhang, B. Wang, H. Dong, et al., "A Strong, Biodegradable, Brush Written all-Wood-Based Flexible Electronic Device," *Cellulose* 31 (2024): 2571–2581, https://doi.org/10.1007/s10570-024-05770-7.

20. H. Ma, C. Liu, Z. Yang, et al., "Programmable and Flexible Wood-Based Origami Electronics," *Nature Communications* 15 (2024): 9272, https://doi.org/10.1038/s41467-024-53708-1.

21. M. Ritter, L. Stricker, I. Burgert, and G. Panzarasa, "Chemiluminescent Wood," *Carbohydrate Polymers* 339 (2024): 122166, https://doi.org/10.1016/j.carbpol.2024.122166.

22. M. Nogi, S. Ifuku, K. Abe, K. Handa, A. N. Nakagaito, and H. Yano, "Fiber-Content Dependency of the Optical Transparency and Thermal Expansion of Bacterial Nanofiber Reinforced Composites," *Applied Physics Letters* 88 (2006): 133124, https://doi.org/10.1063/1.2191667.

23. S. Ifuku, S. Morooka, A. N. Nakagaito, M. Morimoto, and H. Saimoto, "Preparation and Characterization of Optically Transparent Chitin Nanofiber/(meth)Acrylic Resin Composites," *Green Chemistry* 13 (2011): 1708–1711, https://doi.org/10.1039/c1gc15321h.

24. S. Yildiz, E. D. Gezer, and U. C. Yildiz, "Mechanical and Chemical Behavior of Spruce Wood Modified by Heat," *Building and Environment* 41 (2006): 1762–1766, https://doi.org/10.1016/j.buildenv.2005.07.017.

25. N. Terashima, K. Kitano, M. Kojima, M. Yoshida, H. Yamamoto, and U. Westermark, "Nanostructural Assembly of Cellulose, Hemicellulose, and Lignin in the Middle Layer of Secondary Wall of Ginkgo Tracheid," *Journal of Wood Science* 55 (2009): 409–416, https://doi.org/10.1007/s10086-009-1049-x.

14392054, 2026, 2, Downloaded from https://onlinelibrary.wiley.com/doi/10.1002/mame.202500389 by The University Of Osaka, Wiley Online Library on [11/02/2026]. See the Terms and Conditions (https://onlinelibrary.wiley.com/terms-and-conditions) on Wiley Online Library for rules of use; OA articles are governed by the applicable Creative Commons License